

Selective removal mercury (II) from aqueous solution using silica aerogel modified with 4-amino-5-methyl-1,2,4-triazole-3(4H)-thion

Fariba Tadayon^{*†}, Mohammad Saber-Tehrani^{**}, and Shiva Motahar^{*}

^{*}Department of chemistry, North Tehran Branch, Islamic Azad University, Tehran, Iran

^{**}Department of chemistry, Science and Research Branch, Islamic Azad University, Tehran, Iran

(Received 7 November 2011 • accepted 9 October 2012)

Abstract—Silica aerogel surface modifications with chelating agents for adsorption/removal of metal ions have been reported in recent years. This investigation reported the preparation of silica aerogel (SA) adsorbent coupled with metal chelating ligands of 4-amino-5-methyl-1,2,4-triazole-3(4H)-thion (AMTT) and its application for selective adsorption of Hg(II) ion. The adsorbent was characterized by Fourier transform infrared spectra (FTIR) and thermo gravimetric analysis (TGA) measurements, nitrogen physisorption and scanning electron microscope (SEM). Optimal experimental conditions including pH, temperature, adsorbent dosage and contact time have been established. Langmuir and Freundlich isotherm models were applied to analyze the experimental data. The best interpretation for the experimental data given by the Langmuir isotherm equation and the maximum adsorption capacity of the modified silica gel and silica aerogel was 142.85 and 17.24 mgg⁻¹, respectively. Thermodynamic parameters such as Gibbs free energy (ΔG°), standard enthalpy (ΔH°) and entropy change (ΔS°) were investigated. The adsorbed Hg(II) on the SA-AMTT adsorbents could be completely eluted by 1.0 M KBr solution and recycled at least four times without the loss of adsorption capacity. The results of the present investigation illustrate that modified silica aerogel with AMTT could be used as an adsorbent for the effective removal of Hg(II) ions from aqueous solution.

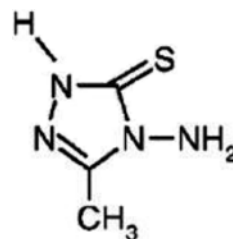
Key words: Mercury, Silica Aerogel, Removal, Selectivity, Adsorption

INTRODUCTION

Aqueous heavy metal pollution represents an important environmental problem due to its toxic effects and accumulation throughout the food chain. Mercury is one of the most toxic metals found in the environment [1,2]. In the European Union, 1 $\mu\text{g L}^{-1}$ as the maximum mercury concentration is allowed in drinking water. Therefore, a very low concentration of mercury in water is very toxic [3]. Long-term effect of Hg(II)-contaminated water causes damage of the central nervous system, impairment of kidney function, chest pain and dyspnoea [4]. Mercury cycles in the environment as a result of natural sources, such as volcanic emissions, and human activities like mining, waste incineration and industrial processes where chloro-alkali process and manufacture of batteries, lamps, paints, and paper are prominent [5]. Industrial and municipal wastewaters are main sources of Hg(II) contamination in natural water [6]. Therefore, it is crucial to remove Hg(II) from wastewater before discharge.

Technologies like precipitation [7], ion exchange [8], amalgamation [9], coagulation [10], membrane separation [11], and adsorption [12] are reported for Hg(II) removal from water. Adsorption technology has been widely accepted because of its effectiveness, flexibility in design and operation, regeneration of the adsorbent by suitable desorption process and economics [13]. Nanomaterials are highly promising in water purification process due to their unique properties like higher surface area per unit volume, ease with which they can be anchored onto solid matrices and the ability to func-

tionalize with different functional groups to enhance their affinity towards target molecules [14]. Aerogels, nanomaterials normally prepared by sol-gel polymerization and supercritical drying, have great potential for use as adsorbents [15]. Silica aerogels are a highly porous, open cell, low-density foam. Furthermore, one of the most important properties of silica aerogels is also the possibility to modify their surface chemical nature with the incorporation of organic functional groups [16,17]. Silica aerogel (SA) surface modifications with chelating agents for adsorption/ removal of metal ions have been reported in recent years, such as polyacramide [18], mercaptopropyl [19] were successfully incorporated. These materials have demonstrated ability to remove various heavy metal ions such as Cu²⁺, Hg²⁺. In this literature was used 4-amino-5-methyl-1,2,4-triazole-3(4H)-thion (AMTT) as metal chelating ligands (for structure see Scheme 1) and its application for selective adsorption of Hg(II) ion. The present study had two aims: first, we synthesized, silica aerogel (SA) nanoparticles adsorbent coupling with metal chelating ligands of AMTT by sol gel method. Secondly, we studied its application for removal of Hg(II) from aqueous solutions. Various spec-



Scheme 1. The structures of AMTT.

[†]To whom correspondence should be addressed.
E-mail: F_Tadayon@iau-tnb.ac.ir

troscopic and microscopic examinations were done to characterize the material and evaluate its performance for Hg(II) uptake. The thermodynamic functions and adsorption isotherms for Hg(II) ions onto SA-AMTT from aqueous solutions were investigated in a batch system. The effects of the Hg(II) ions concentration, temperature, pH and adsorbent dosage were studied to determine the optimal adsorption conditions. Regeneration and reusability of the supported adsorbent was also studied to evaluate the economics of the adsorbent as the Hg(II) removal medium.

EXPERIMENTAL

1. Materials and Methods

AMTT [20] was prepared according to the method described in previous work. Tetramethoxysilane (TMOS) and methyltrimethoxysilane (MTMS) from Aldrich and other reagents used in the present study were of analytical grade from E.Merck. 1,000 $\mu\text{g mL}^{-1}$ of Hg(II) stock solution was prepared by dissolving 1.354 g of HgCl_2 in 10 mL 1 M HNO_3 and diluted by distilled water. Doubly distilled deionized water was used in all experiments. Diluted HNO_3 and NaOH solutions were used for adjusting the initial pH of solutions. Atomic absorption analysis of the various metal ions was performed with a flame atomic absorption spectrophotometer (Perkin-Elmer, Model 4100, made in Australia, 2004), equipped with a GTA_100 graphite furnace atomizer). An infrared spectrum was obtained using an FT-IR (Bruker, model vertex vo) to identify the functional groups and chemical bonding of the coated materials. The pellets were prepared on a KBr press and the spectra were scanned over the wave number range of 4,000–400 cm^{-1} . Scanning electron microscopy (SEM) was performed to measure the particle size and shape (SEM-EDX, XL30 and Philips Netherland). Surface area and porosity were defined by N_2 adsorption-desorption porosimetry (77 K) using a porosimeter (Bel Japan, Inc.). The thermal behavior of the dried materials was examined using TGA (Mettler-851e). The pH values were controlled with a Seven Multi pH meter, Mettler Toledo Instruments (Shanghai) Co. Ltd., China.

2. Adsorbents Synthesis

The 5.02 mL TMOS was diluted with 44.2 mL of methanol, then 1.5 mL of MTMS was added and finally 1.2 mL NH_4F (0.1 mol L^{-1}) solution was added to mixture. Then the mixture was stirred at 20 °C for 30 minutes. After the intermediate product was homogenized by homogenizer (20,000 rpm) and during the homogenization 0.033 g AMTT was added to the mixture. The mixture was poured into a Teflon beaker where the sol aged into hydrogel within about 10 min. After gelation, the gel was left for one day. Subsequently, the product was thoroughly immersed into methanol for 24 h and dried at room temperature for five days and finally the SA-AMTT adsorbent was obtained.

3. Batch Sorption Experiments

Hg(II) batch adsorption experiments were performed in glass conical flasks. 100 mg of SA-AMTT was added to 20 mL of an Hg(II) aqueous solution. The flasks were kept for shaking at 200 rpm in an orbital shaker (Riviera, India) for 24 h. Then the samples were centrifuged at 2,500 rpm for 5 min to separate the adsorbent. The concentration of Hg(II) was determined by Atomic Absorption Spectrometry. The adsorption capabilities can be calculated by the following equation:

$$q_e = (C_i - C_e)V/m \quad (1)$$

Where q_e is the quantity of Hg(II) adsorbed (mg g^{-1}), C_i and C_e are the initial and equilibrium liquid-phase concentrations of Hg(II) (mg L^{-1}), respectively, V is the volume of the solution (L) and m is the quantity of adsorbent used (g). The dosage of the adsorbent was studied in the 20–100 mg range, Hg(II) uptake was also investigated as a function of pH by varying it from around 2–11 and at an initial Hg(II) concentration of 20 mg L^{-1} . Equilibrium studies were performed as a function of temperature (20, 35, 45 and 60 °C). The initial Hg(II) concentration was studied between 10 and 300 mg L^{-1} .

4. Adsorption Isotherm

The more common models were used to investigate the adsorption isotherm Langmuir, Freundlich equations. So, the experimental results of this study were fitted with these two models. Isotherm studies were carried out with initial concentrations of Hg(II) ranging from 20 mL of 10 to 300 mg L^{-1} and pH of the solutions was adjusted to 6.0. The adsorption process was conducted with stirring for 8 h at different temperatures (20, 45 and 60 °C).

5. Desorption Studies

Desorption studies can help to regenerate the adsorbents, and then can be reused to adsorb Hg(II). For desorption experiments, 0.1 g of SA-AMTT was used for adsorbing Hg(II) in 20 mL of Hg(II) solution (20.0 mg L^{-1}) at pH 6.0. Then the obtained solid-phase mass was shaken to 10 mL 1 M of KBr, KSCN, $(\text{NH}_4)_2\text{CS}$, DDTC for 8 h. The metal recovery was calculated by the following Eq. (2)

$$\text{Recovery (\%)} = \frac{\text{amount of desorbed Hg(II)}}{\text{amount of adsorbed Hg(II)}} \times 100 \quad (2)$$

RESULTS AND DISCUSSION

1. Characterization of Adsorbents

Specific surface area (SSA) is commonly reported as BET surface areas obtained by applying the theory of Brunauer, Emmett, Teller (BET) to nitrogen adsorption/desorption isotherms measured at 77 K. The specific surface area of the sample is determined by physical adsorption of a gas on the surface of the solid and by measuring the amount of adsorbed gas corresponding to a monomolecular layer on the surface [21,22]. The results of the method showed that the average specific surface area of SA-AMTT was 589 m^2g^{-1} . It was noticed that the existence of the AMTT network reduced the SSA of the SA-AMTT to 589 m^2g^{-1} compared to the silica aerogel having an SSA equal to 623 m^2g^{-1} . Fig. 1(a) and (b) shows the SEM micrographs of the SA and SA-AMTT. Silica aerogel particles range between 10–55 μm ; SA-AMTT particles are between 30–100 μm .

The result of TGA shows that there is a very little weight loss up to 300 °C. A further increase of temperature causes weight loss along with exothermic peaks corresponding to the oxidation of surface organic (C) groups. This is the reason why samples became hydrophilic after heating above a temperature of around 300 °C.

In Fig. 2, the FTIR investigation of silica aerogels modified with SA-AMTT is shown in comparison to unmodified silica aerogel. The broad absorption band in the region 3,440–3,435 cm^{-1} and band at 1,636–1,642 cm^{-1} respectively to the adsorbed water and surface silanol groups [23]. The silica aerogel exhibits bands in the 1,250–1,050 cm^{-1} region and 800 cm^{-1} and 457 cm^{-1} easily attributed to the Si-O-Si asymmetric and symmetric stretching vibrations of the

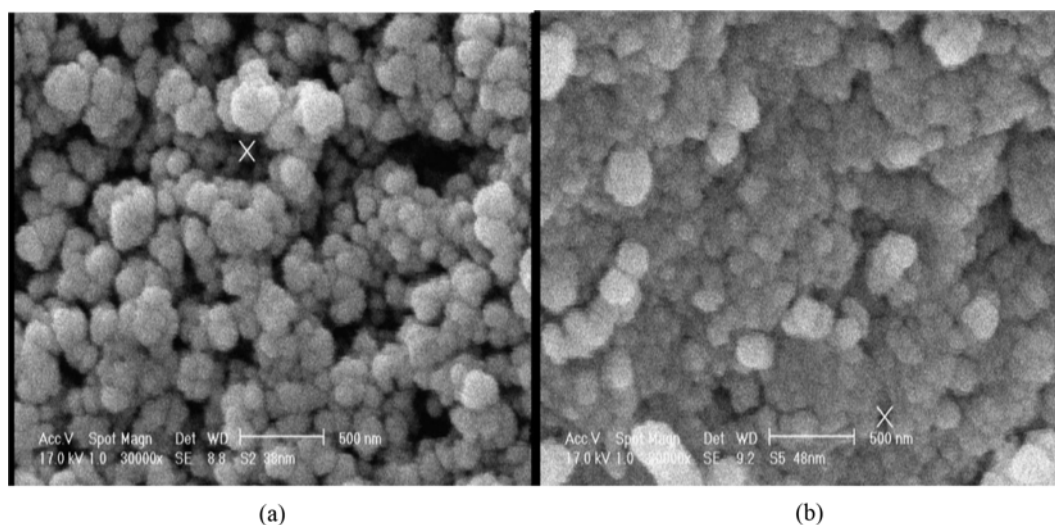


Fig. 1. The SEM image of (a) SA and (b) SA-AMTT.

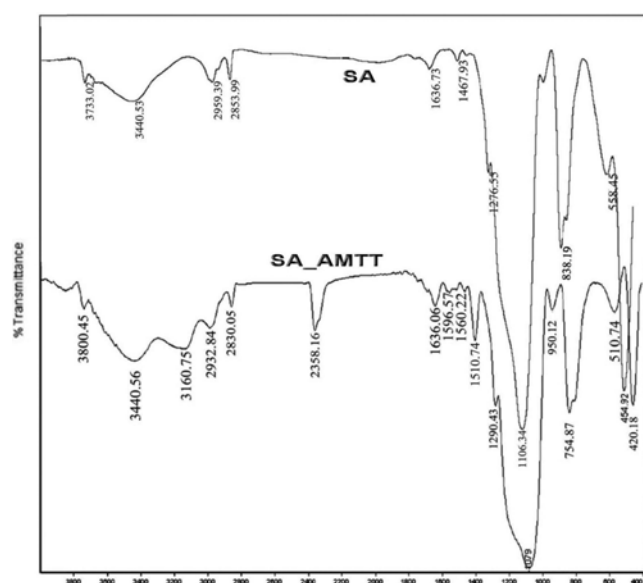


Fig. 2. FTIR absorption spectra of aerogel samples SA, SA-AMTT.

silica network, respectively [24]. The strong and broad peaks obtained for SA-AMTT samples at $1,100\text{ cm}^{-1}$ appear due to Si-OR group and at lower wavelength peaks appear due to asymmetric, symmetric and the bending modes of SiO_2 , respectively, as in the case of unmodified silica aerogel. As expected for SA-AMTT samples, a new but weak and sharp peak appeared at $2,560\text{ cm}^{-1}$ due to sulfur-containing groups [19]. Also, a new but weak and sharp peak appeared at $1,560.22\text{ cm}^{-1}$ due to NH_2 groups, 754 cm^{-1} due to C=S groups, $1,596.57\text{ cm}^{-1}$ is due to N=N stretching vibration [24-26]. This peak is not observed for silica aerogel. Peaks at around $1,600\text{ cm}^{-1}$ and $3,400\text{ cm}^{-1}$ on both graphs correspond to O-H stretching, provided that they are sharper in the case of unmodified silica, which contains more O-H groups. These two peaks are the weakest in the case of SA-AMTT sample, where the amount of precursor mercapto and amino is increased. The above FTIR data indicates that strong interaction exists on the interface of silica aerogel and SA-AMTT, and silica aerogel is successfully modified by AMTT.

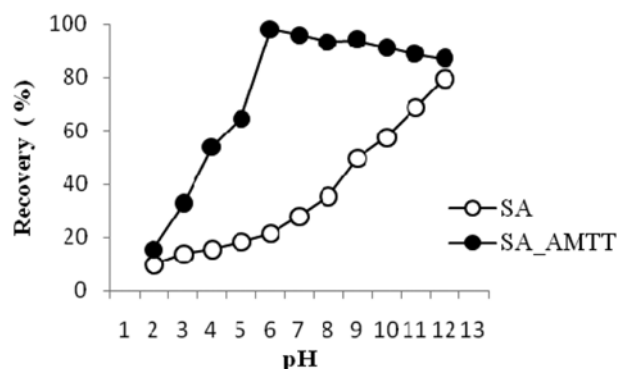


Fig. 3. Effect of pH on adsorption of mercury(II) ions ($[\text{Hg}^{2+}]_0 = 10\text{ mg L}^{-1}$; contact time=20 h; mass of adsorbent=100 mg; solution volume=20 mL).

2. Adsorption Studies

2-1. Effect of pH on Adsorption

Since the binding of metal ions by surface functional groups was strongly pH dependent, the pH of the aqueous solution is an important controlling parameter in the adsorption process [27]. To establish the effect of pH on the sorption of Hg(II) ions onto SA-AMTT and SA, batch equilibrium studies at different pH values were carried out in the range of 2.0-11.0. The experimental results are presented in Fig. 3. As silica has a point of zero charge around 2.5, the adsorbent exhibits a positive zeta potential at pH lower than this value. Therefore, the surface will be positively charged at this pH, which reduces the adsorption due to the electrostatic repulsion between the surface and the mercury cations. The adsorption increases as the pH increase due to the increase of the silica surface negative charges favoring the electrostatic attraction between the two entities with opposite charges, SiO^- and Hg^{2+} [18].

For SA-AMTT: between pH values 3.0 and 7.0 the metal sorption increases sharply, reaching values that remain almost constant for pH values in the range of 7.0-9.0. At lower pH (<6), Hg(II) was in the free ionic form of Hg^{2+} [28], and the positively charged hydrogen ions may have competed with the Hg^{2+} for binding sites on the amino groups on the surface of the SA-AMTT. Once the amino

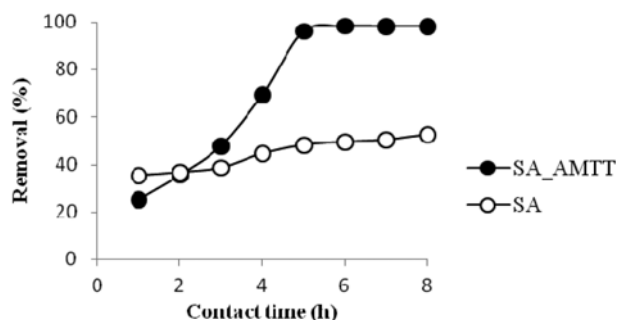


Fig. 4. Evolution of adsorbed quantity of mercury(II) with time ($[Hg^{2+}]_0=20 \text{ mg L}^{-1}$; mass of adsorbent=100 mg; solution volume=20 mL; pH=6; 20 °C).

groups were protonated, the strong electrical repulsion prevented Hg^{2+} from contacting the surface of the SA-AMTT, resulting in lower adsorption capacities at lower pH, and this may be attributed to the decreased solubility of Hg(II) at high pH. At lower pH (>6) the surface of SA-AMTT was negatively charged, which decreased negatively surfactant coating through electrostatic force of repulsion. Therefore, adsorption decreases at pH values higher than 6. So, the optimal pH values to remove Hg(II) by SA-AMTT, 6.0 were used for the adsorption processes in this study.

2-2. Effect of Contact Time

The sorption of Hg(II) by SA-AMTT at various contact times ranging from 5 min to 20 h was performed. As shown in Fig. 4, the removal rate of Hg(II) was completed after almost 8 h, and after this period, the concentration of adsorbed Hg(II) ions did not significantly change further with time. The maximum uptake of Hg(II) ($C_0=20 \text{ mg L}^{-1}$) after the mentioned contact time by the treated SA-AMTT at pH 6.0 was obtained as 98.3%. According to these results, a contact time of 8 h in was set order to ensure that equilibrium conditions were reached.

2-3. Effect of Temperature on Mercury Adsorption Capacity

The effect of the solution temperature on the adsorption capacity was investigated for Hg(II) ions solutions at initial metal concentration 20 mg L^{-1} and adsorbent dose 100 mg. Four different temperatures of 20, 35, 45 and 60 °C were considered. From Fig. 5, it can be observed the removal percent was decreased for Hg(II) ions.

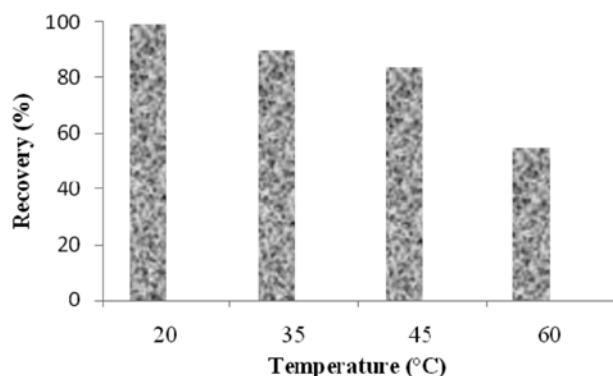


Fig. 5. Influence of temperature on mercury(II) adsorption ($[Hg^{2+}]_0=20 \text{ mg L}^{-1}$; mass of adsorbent=100 mg; contact time=8 h; solution volume=20 mL; pH=6).

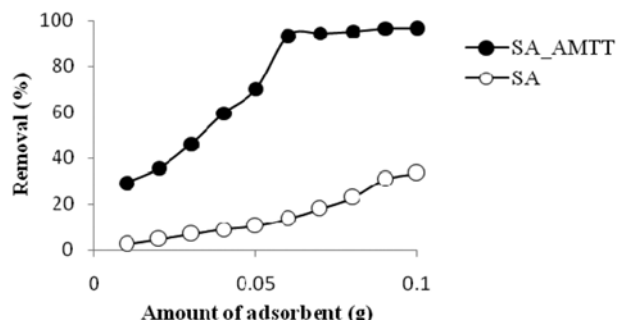


Fig. 6. Influence of adsorbent dose on mercury(II) adsorption ($[Hg^{2+}]_0=20 \text{ mg L}^{-1}$; contact time=8 h; solution volume=20 mL; pH=6; 20 °C).

It decreased from 98.3% to 54.35% when temperature was increased from 20 to 60 °C. These results indicate that the adsorption of Hg(II) ions was exothermic in SA-AMTT [29].

2-4. Effect of Adsorbent Dose

The effect of the quantity of SA-AMTT on the enrichment-recovery of Hg(II) was investigated and the results are shown in Fig. 6. To investigate this effect, several quantities of these adsorbents were tested, which masses between 10 and 100 mg were used per experiment. It was observed that quantitative removals of the mercury ions were attained for adsorbent dosages of at least 60 mg, and for adsorbent dosages higher than these values, the mercury ions removal remained almost constant. Increase in adsorption with increase in adsorbent dosage was attributed to the availability of larger surface area and more adsorption sites. We noticed that 100 mg of SA-AMTT were able to adsorb 96.75% of the quantity of Hg(II) in the solution, while a similar mass of SA was not able to adsorb 33.45% of the initial Hg(II) ions. The quantity of SA-AMTT was both fixed at 100 mg in the following experiments.

2-5. Selectivity

Each of the metal ions such as (Cu(II), Mn(II), Cr(III), Co(II), Cd(II), Ni(II), Fe(II), Zn(II), Pb(II), Al(III)) were set at pH value 6 (the optimum pH for Hg(II) removal). Then in flasks, 0.1 g SA-AMTT added to sample solutions. The flasks were kept for shaking at 200 rpm in an orbital shaker for 6 h. Then the samples were centrifuged at 2,500 rpm for 5 min to separate the adsorbent and the residual concentration of metal ions in the filtrate measured by

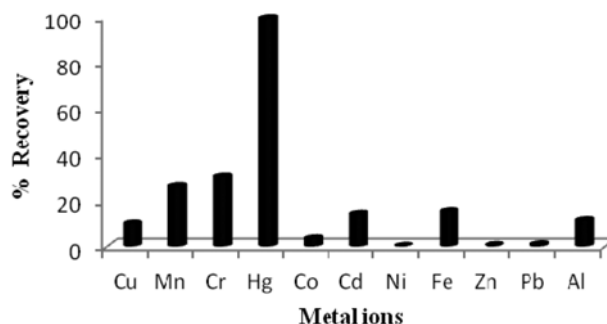


Fig. 7. The effect of using different heavy metal ions on percent removal of heavy metals by SA-AMTT ($[metals]_0=20 \text{ mg L}^{-1}$; pH=6.0; contact time=20 h; mass of adsorbent=100 mg; solution volume=20 mL).

Atomic Absorption Spectrophotometer. From Fig. 7, it's obvious that fewer metal ions can be adsorbed on SA-AMTT in optimum conditions. Therefore SA-AMTT can be used for selective adsorption of Hg(II) in aqueous solution by metal chelating ligand of 4-amino-5-methyl-1,2,4-triazole-3(4H)-thion (AMTT) as selective-ligand. SA-AMTT is the best adsorbent for the removal of Hg(II) ions.

3. Adsorption Isotherms

The Langmuir [30], Freundlich [31] and Dubinin-Radushkevich (DR) models have been tested in this study. The most widely used Langmuir equation, which is valid for monolayer sorption on a surface with a finite number of identical sites, is given by

$$C_e/q_e = 1/q_{max} + 1/q_{max} C_e \quad (3)$$

Where q_{max} is the monolayer capacity of the adsorbent (mg g^{-1}) and b is the Langmuir equilibrium constant (L mg^{-1}). By using the linear form of this isotherm, the plot of C_e/q_e versus C_e gives a line with a slope of $1/q_{max}$ and b were determined, respectively, from the slope and intercept of the plots (Fig. 8(a)). The essential characteristics and the feasibility of the Langmuir isotherm can be explained in terms of a dimensionless constant separation factor or equilibrium param-

eter R_L , which is defined by

$$R_L = 1/(1 + bC_0) \quad (4)$$

where b is the Langmuir constant and C_0 is the initial concentration of metal ions. Favorable adsorption is reported when the R_L values are between 0 and 1 [32]. In the present work, the R_L -values of the Hg^{2+} ions adsorption by SA-AMTT are in the ranges of 0.009-0.023. This result shows that the adsorption process is favorable.

The empirical equation used to describe the Freundlich isotherm is given by

$$q_e = K_F C_e^{1/n} \quad (5)$$

and the linear form of the Freundlich isotherm is

$$\log q_e = \log K_F + 1/n \log C_e \quad (6)$$

Where n is the heterogeneity factor and K_F is the Freundlich constant (L g^{-1}), both commonly temperature dependent; n is typically greater than 1 and the larger is its value, the adsorption isotherm becomes more non-linear and the system becomes more heterogeneous [33]. The linearized form of the Freundlich equation allows the determination of n and K_F from a linear plot of $\ln q_e$ versus $\ln C_e$ (Fig. 8(b)).

The Dubinin-Radushkevich (D-R) model was applied to the equilibrium data to determine if sorption had occurred by physical or chemical processes. The D-R adsorption isotherm is represented as:

$$\log_{10} q_e = \log_{10} q_D - 2 B_D R^2 T^2 \log_{10} (1 + 1/C_e) \quad (7)$$

Where q_D is theoretical saturation capacity (mg g^{-1}) and B_D is a constant related to adsorption energy ($\text{mol}^2 \text{K J}^{-2}$), R is the gas constant ($\text{kJ mol}^{-1} \text{K}^{-1}$) and T is the temperature (K). The slope of the plot $\log_{10} q_e$ versus $\log_{10} (1 + 1/C_e)$ gives the q_D and B_D values (Fig. 8(c)). The constant B_D gives an idea about the mean free energy E (kJ mol^{-1}) of adsorption per molecule of the adsorbate when it is transferred to the surface of the solid from infinity in the solution and can be calculated from the D-R isotherm constant B_D using the following equation [34]:

$$E = 1/\sqrt{2B_D} \quad (8)$$

The high values of q_D show high sorption capacity and these are higher for the unmodified than the modified.

The magnitude of E provides information on the nature of the sorption process, i.e., whether it is chemical or physical, with values in the range $E=1-8 \text{ kJ mol}^{-1}$ corresponding to physical sorption and in the range $9-16 \text{ kJ mol}^{-1}$ to chemisorption. The calculated E value was found to be $1.096 \text{ kJ mol}^{-1}$ (Table 1). E value less than 8 kJ mol^{-1} as indicated by our results shows that the adsorption process of Hg(II) on SA-AMTT follows physical adsorption.

A comparison of the coefficient of regression (R^2) for the three isotherms is shown on Table 1.

After comparing the three theoretical models to the experimental data, it was clearly found that the Langmuir isotherm represents the best fit of the experimental results over the other isotherms.

4. Thermodynamic Parameters

The thermodynamic equilibrium constant (K'_C) was obtained by calculating apparent equilibrium constant (K'_C) at different temperature and initial concentration of Hg(II) and extrapolating to zero [35,36].

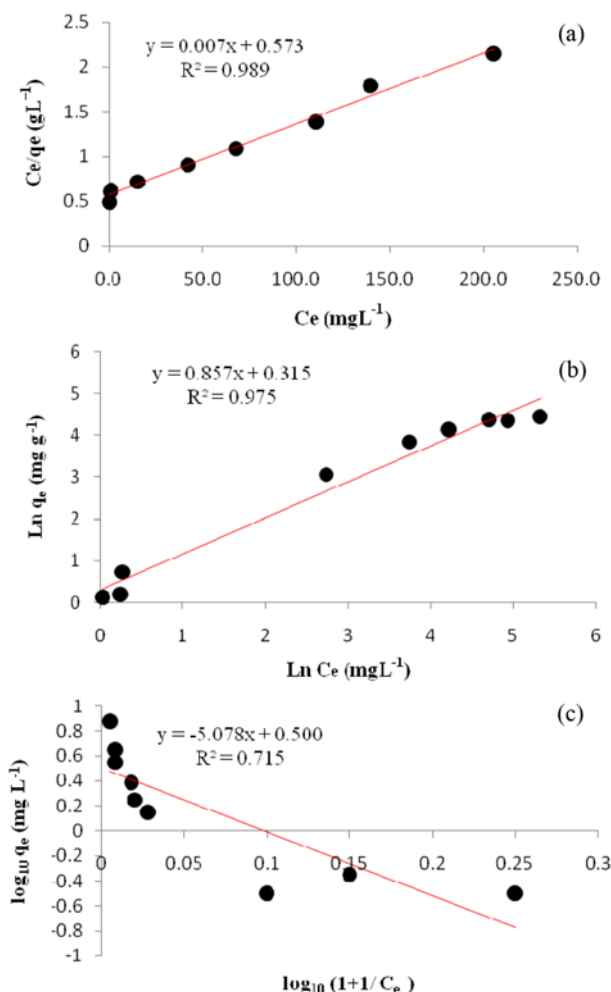


Fig. 8. (a) Langmuir isotherm (b) Freundlich isotherms (c) Dubinin-Radushkevich isotherm on SA-AMTT ($[\text{Hg}^{2+}]_0=10-300 \text{ mg L}^{-1}$; mass of adsorbent=100 mg; contact time=8 h; solution volume=20 mL; pH=6; 20°C).

Table 1. Langmuir, Freundlich and Dubinin-Radushkevich model's regression constants for Hg(II) adsorption on SA-AMTT and SA at different temperatures

Temperature (°C)	Langmuir constants			Freundlich constants			Dubinin-Radushkevich constants			
	q_{max} (mgg ⁻¹)	b (Lmg ⁻¹)	R^2	n	K_F (Lg ⁻¹)	R^2	B_D mol ² KJ ⁻²	q_D mg g ⁻¹	E kJmol ⁻¹	R^2
SA-AMTT										
20 °C	142.85	1.22×10^2	0.989	1.308	5.610	0.975	0.456	1.435	1.096	0.715
45 °C	100	1.88×10^2	0.970	1.736	23.761	0.943	0.392	1.312	1.129	0.702
60 °C	111.11	1.26×10^2	0.981	1.38	0.193	0.973	0.389	1.045	1.133	0.803
SA										
20 °C	17.24	2.08×10^2	0.859	2.469	3.061	0.815	0.125	2.523	2.00	0.775
45 °C	21.27	0.99×10^2	0.873	1.560	0.187	0.955	0.198	2.275	1.589	0.843
60 °C	16.94	1.16×10^2	0.990	1.555	0.133	0.982	0.152	2.154	1.813	0.773

$$K'_c = C_e/C_e \quad (9)$$

The change of Gibbs free energy (ΔG°), enthalpy (ΔH°), and entropy (ΔS°), for the adsorption processes was calculated using the following equations:

$$\ln K'_c = -\Delta H^\circ/RT + \Delta S^\circ/R \quad (10)$$

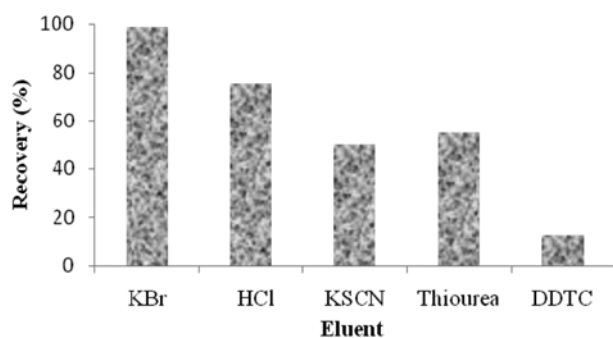
and

$$\Delta G^\circ = -RT \ln K'_c \quad (11)$$

From the slope and intercept of the plot $\ln K'_c$ versus $1/T$, the values of ΔH° and ΔS° had been computed, while ΔG° was calculated using Eq. (11). The obtained thermodynamic parameters are presented in Table 2. The values of ΔG° calculated using the K'_c were negative, which confirms the feasibility of the process and the spontaneous nature of the adsorption. At 293 K the system was spontaneous and spontaneously decreased as the temperature increased. The negative values of ΔH° denote that the process was exothermic. The nega-

Table 2. Thermodynamic parameters for Hg(II) adsorption on SA-AMTT at different temperatures

Temperature (K)	ΔG° (kJ mol ⁻¹)	ΔH° (kJ mol ⁻¹)	ΔS° (kJmol ⁻¹ K ⁻¹)
293	-8.258	-13.809	-0.016
318	-7.746		
333	-7.502		

**Fig. 9. Percentage of mercury recovered by using different eluant ([eluant]=1 M; eluant volume=20 mL; t=24 h; 20 °C).**

tive value of ΔS° suggests the decrease of randomness through the interface during the adsorption of Hg(II) ions onto the surface of SA-AMTT.

5. Desorption Experiments

Desorption studies help elucidate the mechanism of sorption and recover metals from wastewater and sorbent. The results are shown in Fig. 9. Thiourea, and potassium thiocyanate exhibit rather similar behavior in the regeneration process, being that the removed mercury percentages 55% and 50%, respectively. Hydrochloric acid exhibits a better behavior than thiourea, and potassium thiocyanate, removing a slightly higher amount of mercury towards the aqueous solution (65%). It was observed that DDTC promotes remarkable removal of the mercury ions loaded SA-AMTT (75%). The highest desorption was observed for the KBr solution as the effluent (98%). Additionally, to investigate the reusability of the SA-AMTT, three adsorption-desorption cycles were carried out under optimum conditions. The result reveals that SA-AMTT has excellent reuse potential and only 4% reduction in Hg(II) uptake capacity was observed at the end of the third cycle (Table 3), which reveals its great potential to be used as reusable adsorbent for the removal of Hg(II).

CONCLUSIONS

Modified silica aerogel with AMTT, an Hg adsorbent, was synthesized and the adsorption of Hg was investigated in batch technique. FTIR, SEM and TGA were used to characterize the as-prepared SA-AMTT. Adsorption was found to be dependent on Hg(II) concentration, adsorbent dose and pH of the system; the optimum pH was found to be in the range of 6, and the equilibrium time was

Table 3. Performance of fresh and recycled

Cycle ^{a,b}	Recovery (%)	q_e (mgg ⁻¹)
Fresh	85.5±0.20	50.85±0.32
(1 st run)	81.1±0.11	49.41±0.25
(2 nd run)	79.5±0.28	47.67±0.15
(3 rd run)	72.5±0.39	46.20±0.44

^aAdsorption: ammonium initial concentration 30 mgL⁻¹ and adsorption time 8 h

^bDesorption: desorbing solution 1 M KBr and desorption time 24 h

reached within 8 h. Maximum uptake was obtained at adsorbent dose of 0.06 g, which may be considered as optimum adsorbent dosage level at the specified conditions. The adsorption medium temperature had no significant effect on the adsorption capacity between 20 and 60 °C. The negative value of ΔH and negative value of ΔG indicate exothermic and spontaneous nature of sorption, respectively.

Almost all adsorbed Hg on the SA-AMTT adsorbent could be eluted quickly with 1 M KBr. The adsorbents were reused in three adsorption and desorption cycles with negligible decrease (only 4% reduction) in adsorption capacities. The adsorption isotherm was studied, revealing that the adsorption was fitted with the Langmuir model with a monolayer adsorption capacity of 142.85 mgg⁻¹. The results of the present investigation illustrate that modified silica aerogel with AMTT could be used as an adsorbent for the effective removal Hg(II) ions from aqueous solution.

REFERENCES

1. T. S. Anirudhan, L. Divya and M. Ramachandran, *J. Hazard. Mater.*, **157**, 620 (2008).
2. C. Namasivayam and K. Periasamy, *Water Res.*, **27**, 1663 (1993).
3. Directive 2000/60/EC of the European Parliament and of the Council of October 23 (2000). (L327 of 22-12-2000).
4. R. Say, E. Birlik, Z. Erdemgil, A. Denizli and A. Ersoz, *J. Hazard. Mater.*, **150**, 560 (2008).
5. United Nations Environment Programme: Chemicals, Global Mercury Assessment, Geneva, Switzerland, December (2002).
6. H. Von Canstein, Y. Li, K. N. Timmis, W. D. Deckwer and I. Wagner-Döbler, *Appl. Environ. Microbiol.*, **65**, 5279 (1999).
7. M. M. Matlock, B. S. Howerton and D. A. Atwood, *Water Res.*, **36**, 4757 (2002).
8. D. Kratochvil and B. Volesky, *Water Res.*, **32**, 2760 (1998).
9. K. P. Lisha and A. T. Pradeep, *Gold Bull.*, **42**, 58 (2009).
10. Y. Terashima, H. Ozaki and M. Sekine, *Water Res.*, **20**, 537 (1986).
11. A. Oehmen, R. Viegas, S. Velizarov, M. A. M. Reis and J. G. Crespo, *Desalination*, **199**, 405 (2006).
12. T. Budinova, N. Petrov, J. Parra and V. Baloutzov, *J. Environ. Manage.*, **88**, 165 (2008).
13. K. P. Lisha, M. Maliyekkal and T. Pradeep, *Chem. Eng. J.*, **160**, 432 (2010).
14. Pradeep, Anshup T., *Thin Solid Films*, **517**, 6441 (2009).
15. C.-T. Wang and S.-H. Ro, *Appl. Catal. A: General*, **285**, 196 (2005).
16. R. T. Yang, *Adsorbents: Fundamentals and applications*, Wiley-Interscience (2003).
17. D. M. Ruthven, *Principles of adsorption and adsorption processes*, Wiley-Interscience (1984).
18. H. Ramadan, A. Ghanem and H. El-Rassy, *Chem. Eng. J.*, **159**, 107 (2010).
19. S. Štandeker, A. Veronovski, Z. Novak and Ž. Knez, *Desalination*, **269**, 223 (2011).
20. A. Dornow, H. Menzel and P. Marx, *Chem. Ber.*, **97**, 2173 (1964).
21. S. Brunauer, P. H. Emmett and E. Teller, *J. Am. Chem. Soc.*, **60**, 309 (1938).
22. K. S. Walton and R. Q. Snurr, *J. Am. Chem. Soc.*, **129**, 8552 (2007).
23. G. Socrates, *Infrared and raman characteristic group frequencies: Tables and charts*, 3rd Ed., John Wiley & Sons (2001).
24. A. Duran, J. M. Fernandez Navarro, P. Casariego and A. Joglar, *J. Non-Cryst. Solids*, **82**, 391 (1986).
25. O. Estevez-Hernandez and E. Otazo-Sanchez, *Spectrochim. Acta Part A*, **62**, 964 (2005).
26. O. Estevez-Hernandez, E. Otazo-Sanchez, J. L. Hidalgo-Hidalgo de Cisneros, I. Naranjo-Rodriguez and E. Reguera, *Spectrochim. Acta Part A*, **64**, 961 (2006).
27. M. M. Rao, A. Ramesh, G. P. C. Rao and K. Sessaiah, *J. Hazard. Mater.*, **129**, 123 (2006).
28. Y. P. Kunar, P. King and V. S. R. K. Prasad, *Chem. Eng. J.*, **129**, 161 (2007).
29. S. D. Khattri and M. K. Singh, *J. Hazard. Mater.*, **167**, 1089 (2009).
30. I. Langmuir, *J. Am. Chem. Soc.*, **40**, 1361 (1918).
31. H. Freundlich, *T. Faraday Soc.*, **28**, 195 (1932).
32. Mouzdahir Y. El, A. Elmchaouri, R. Mahboub, A. Gil and S. A. Korili, *J. Chem. Eng. Data*, **52**, 1621 (2007).
33. D. D. Duong, *Adsorption analysis: Equilibria and kinetics*, Imperial College Press, London (1998).
34. M. Horsfall, A. I. Spiff and A. A. Abia, *B. Korean Chem. Soc.*, **25**, 969 (2004).
35. A. K. Bhattacharya, T. K. Naiya, S. N. Mandal and S. K. Das, *Chem. Eng. J.*, **137**, 529 (2008).
36. B. Singha and S. K. Das, *Colloids Surf. B.*, **84**, 221 (2011).